Received Signal Strength Based Gait Authentication

Marshed Mohamed and Michael Cheffena

***Abstract*—Expansion of wireless body area networks (WBANs) applications such as health-care, m-banking, and others has lead to vulnerability of privacy and personal data. An effective and unobtrusive natural method of authentication is therefore a necessity in such applications. Accelerometer-based gait recognition has become an attractive solution, however, continuous sampling of accelerometer data reduces the battery life of wearables. This paper investigates the usage of received signal strength indicator (RSSI) as a source of gait recognition. Unlike the accelerometer-based method, the RSSI approach does not require additional sensors (hardware) or sampling of them, but uses the RSSI values already available in all radio devices. Three radio channel features namely, the time series, auto-correlation function, and level crossing rate were extracted from unique signature of the RSSI in relation to the corresponding subject. The extracted features were then used together with 4 different classification learners namely decision tree, support vector machine, k-nearest neighbors, and artificial neural network, to evaluate the method. The best performance was achieved utilizing artificial neural network with 95% accuracy when the features were extracted from 1 on-body radio channel (right wrist to waist), and 98% when the features were extracted from 2 on-body radio channels (right wrist to waist, and left wrist to waist). The developed RSSI-based gait authentication approach can complement high-level authentication methods for increased privacy and security, without additional hardware, or high energy consumption existing in accelerometer-based solutions.**

***Keywords*—Wireless body area networks, physical layer security, wireless channel characteristics, biometrics authentication, human gait.**

I. Introduction

THE advances in microelectronics and wireless communications have led to the availability of lightweight devices with wireless communication capabilities that can be used to monitor the human body functions and its surrounding environment. Networks made of such devices are known as Wireless Body Area Networks (WBANs) and have found significant applications in health monitoring [1]. In such applications, WBAN sensors collect vital physiological parameters of a subject, which serve as a reference in medical diagnosis, treatment and health indicator in industry service as well. Due to the sensitivity of the data involved, security and privacy measures are vital to the success of the WBANs [2].

Due to the difficulty for biometrics counterfeit, biometrics authentication has been proposed as a solution to improve security in the communication of such personal data [3]. One of the biometric traits which is attractive in health monitoring applications security is gait. Studies in medicine and psychology have shown that each individual has a distinctive walking style that allows his recognition. Unlike other biometrics traits such as voice, fingerprints, and facial recognition, gait is non-invasive and can be measured without subject intervention. This makes it more user-friendly especially in continuous identity re-verification [4].

Although the first gait recognition systems used video, the current trend is to use accelerometers included in wearables or portable smart devices [5]. In [6] a real-time gait recognition system using the wavelet transform was presented. The simulation results showed that the proposed method has reliable recognition accuracy both in the real-time and in the long-term cases. Machine learning algorithms were used in [7] to train the classifiers and authenticate the subjects. More specifically their work concentrates on methods of segmentation of the accelerometer data and compares between the fixed length and fixed cycle approach in which fixed length showed better results. Further research was conducted in [8] on the influence of walking speeds and surfaces on gait recognition. Different parameter settings in dynamic time warping were evaluated to optimize the cycle extraction process. Since most methods on accelerometer-based gait recognition suffer from cycle detection failures, [4] proposed a novel algorithm which uses a multiscale signature point extraction method, and has shown significant improvements.

accelerometer-based gait recognition systems have a lot of positive traits, however, they suffer from high energy consumption due to continuous accelerometer data sampling. Researcher in [9] tried to solve this problem by proposing a kinetic energy harvesting device and used its output voltage signal as the source of gait recognition. In [10] capacitive coupled human body communication was presented as a biometric authentication method instead. The method requires S-parameters over wide range of frequencies to be able to function. With the use of current available devices, [11]–[13] attempts to exploit propagation characteristics or wireless channel to obtain behavioral fingerprint and use it in authentication. They make use of the channel state information (CSI) of Wi-Fi signal to extract features that identify individuals by their intrinsic body movement during walking without attachments to the body. It requires a multiple antenna transmitter and receiver fixed in a certain environment.

In this work a received signal strength indicator (RSSI) based gait authentication method is proposed. Arm movement during walking has been chosen as the gait identification feature as the body mounted sensors on the arm wrists (smartwatches) are already popular. The method does not require hardware upgrades as it only relies on regular communication between body mounted sensors (e.g. smartwatch) and body mounted access node (e.g. smartphone). This makes the system mobile and not bounded to a specific location, contrary to Wi-Fi-based gait recognition systems. Unlike accelerometer-based

M. Mohamed, and M. Cheffena, are with the Norwegian University of Science and Technology, Gjøvik, Norway (e-mail: marshed.mohamed@ntnu.no, michael.cheffena@ntnu.no).

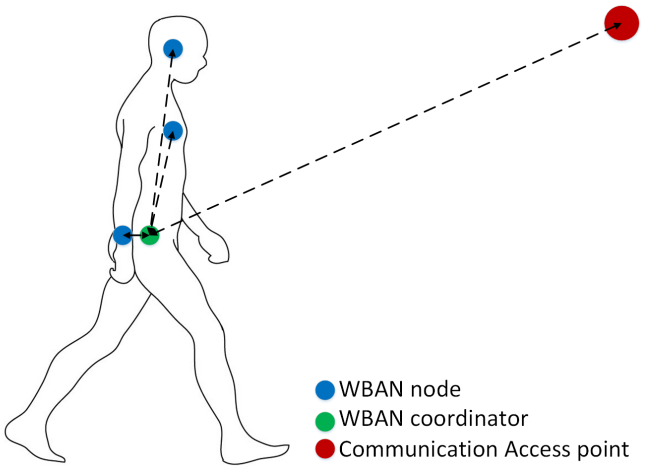

Fig. 1. Example of WBAN with 3 nodes and 1 coordinator. The off-body node act as communication access point.

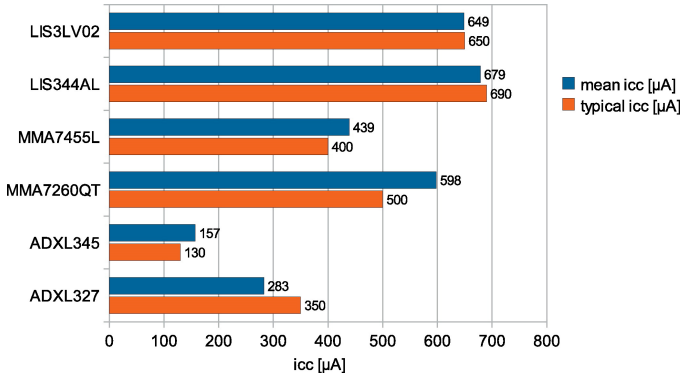

Fig. 2. Mean current consummation of common accelerometers connected to 3.3 V power supply together with typical values given in their respective data sheets [16].

gait recognition systems, it does not require sampling of sensor data, making it more energy efficient. Moreover, it does not require any additional packet transmission but instead, make use of the RSSI values available in regular communications.

The paper begins in Section II by discussing the radio features that are applicable in gait detection. In Section III, 4 different classification learners are presented for use in RSSI-based gait authentication. Experimental data and performance analysis is presented in Section IV. Finally, the conclusion is given in Section V.

II. Gait Radio Features

The most common architecture of WBANs consist of body-mounted sensors known as nodes, and an access node such as smartphone also mounted on the body, known as central coordinator as shown in Fig. 1 [14]. The nodes have sensors that measure various physiological conditions, or other types of data and transmit it wirelessly to the coordinator. The coordinator acts as an access point by collecting data from the nodes, and transmit them to the data center through an off-body node acting as a communication access point. It is in the radio channel between the nodes and the coordinator that the gait information is available and could be extracted, processed and used for authentication by the coordinator. If processing power is a concern at the coordinator, the raw gait information could simply be forwarded to the server together with the rest of the data, and the authentication process could be performed there. This kind of authentication will ensure that the data uploaded to the server are indeed from the intended subject and will prevent impersonation attacks. It could be used together with other authentication methods, to add another security layer for applications in which one-time validation of the user's identity is insufficient. Since it can be measured without subject intervention, it could be used as a continuous authentication method and set to trigger other security measures whenever it fails.

The gait information available in the radio channels can be extracted from the measurement of the power present in the received signal. This measurement is already being conducted by wireless radio transceivers and is indicated by their RSSI values [15]. This gives the RSSI method an edge over the accelerometer-based systems, which needs sampling of sensor data specifically for gait recognition purpose. The most commonly available accelerometers have been shown to consume current of more than 130μA [16] as shown in Fig 2, and that the sampling process consumes around 3 mW for low power processors [9] and 370 mW for smartphones [17]. The proposed method eliminates the sensor, and all the power consumption related to it by relying on measurement which are already conducted by transceivers and are available for processing. This means the power consumption on the sensor node (e.g., smartwatch) due to RSSI based method is zero. The RSSI values are used to obtain radio features such as variation of power received with time (time series), the measure of degree of time dependency (auto-correlation function), and how often does the signal crosses a certain threshold (level crossing rate). It is through these radio features that one subject can be differentiated from the other. The considered radio features are discussed in the following.

A. The Time Series

It has been shown that the power received in a WBANs is related to the dynamics involved with the specific activity of the subject . For the case of walking, the power received is periodic to the relative movement of the body parts where the nodes are attached to. The period of the signal tends to correspond to the period of the limb swinging, and the amplitude variation depends on the size of the limbs, distance from its rest position, and the amount of shadowing the body provide during walking [18]. This is normally different enough from one person to another to a point that it could be used for individual identification.

Fig. 3. shows the time series of the received signal power of 3 subjects during walking for the duration of 3 seconds. The transceivers were placed at the right wrist and the right side of

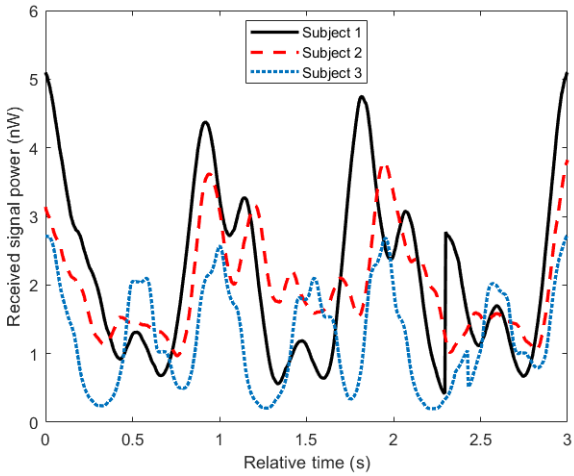

Fig. 3. Example of time series of the received signal power of WBANs of 3 different subjects during walking. The transmitter was attached to the waist, and the receiver was attached to the right wrist.

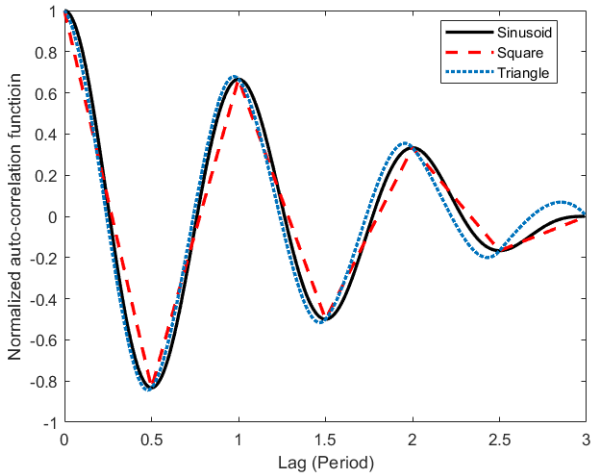

Fig. 4. Example of normalized ACF of periodic signals of length of 3 periods. The ACF of all the signals have peaks at $\tau = 1$ of $\frac{2}{3}$, and at $\tau = 2$ of $\frac{1}{3}$

the waist, and the received signal power was smoothed using a sliding window of length of 0.15 seconds. The time series of all 3 subjects are periodic with a period of around 1 second, consistent with the oscillatory movement of the corresponding arms. However, the series also show that the received signal power is different between the subjects and hence, the overall patterns have enough features to distinguish them from one another. More discussions on the measurement campaign and the subjects involved are provided in Section IV.

B. The Auto-Correlation Function

The Auto-correlation function (ACF) is a measure of the degree of time dependency among the observations of signals. It is used to characterize the periodicity in a fading signal envelope. For real discrete sampled data $x(t)$, it can be calculated using [19], [20]:

$$r_{xx}(\tau) = \sum_{t=1}^{N-\tau} (x(t) - \mu)(x(t-\tau) - \mu) \tag{1}$$

where τ is the time delay, N is the length and μ is the mean of the sampled data. The normalized ACF can then be obtained by using (2) to give an output with a maximum value of 1 at $\tau = 0$

$$\rho_{xx}(\tau) = \frac{r_{xx}(\tau)}{r_{xx}(0)} \tag{2}$$

For a perfect periodic signal, the normalized ACF oscillates with its period corresponding to the period of the signal. If the signal is limited to a specific number of periods (it does not go to infinity), the envelope of the normalized ACF tends to decay exponentially. Take for example the normalize ACF of periodic signal limited to 3 periods will have a peak of 1 at $\tau = 0$, a peak of $\frac{2}{3}$ at $\tau = 1$ period, and a peak of $\frac{1}{3}$ at $\tau = 2$ periods as shown in Fig. 4 for sinusoid, square, and triangle signals. These peaks values tend to decrease as the noise in the

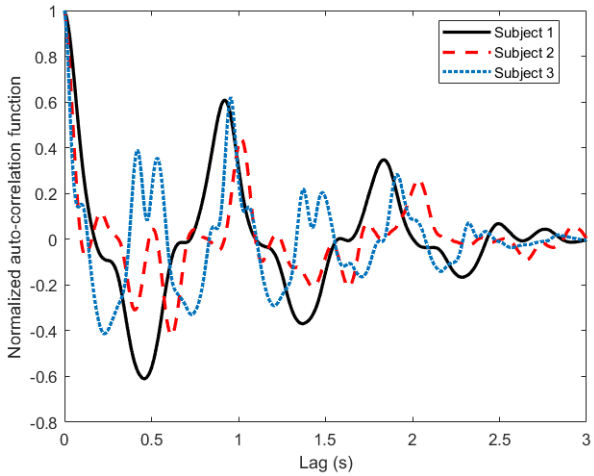

Fig. 5. The normalized ACF of the signals shown in Fig.3. The ACFs show properties of periodic signals with significantly different patterns.

periodic signal increase and hence can be used as an indicator of change in activity. Take for example if a walking subject stops in the middle of sampling, the peak value at $\tau = 1$ period will be significantly smaller than the expected value and hence the change in activity could be detected.

In addition to that, since the received signal power is different from one subject to the other during walking, the normalized ACF has the potential of being different. Fig. 5 shows the normalized ACF of the signals shown in Fig. 3. The ACF of the 3 subjects show properties of a signal composed from a number of periodic signals, with the main envelope having a period of around 1s (0.92 s for Subject 1, 1.02 s for Subject 2, and 0.96 s for Subject 3), consistent with the oscillatory movement of the corresponding arms. However, the composition of these periodic signals are different from

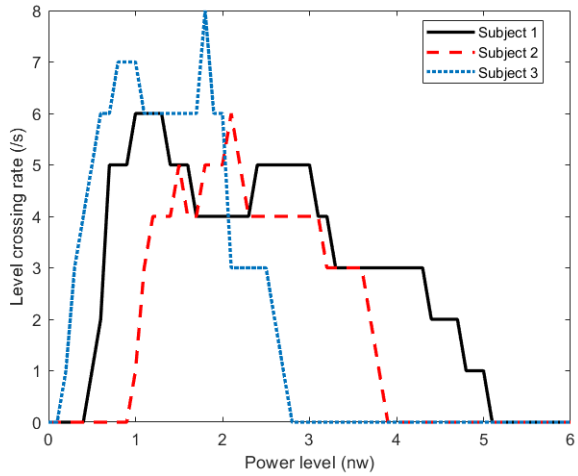

Fig. 6. LCR representation of signals shown in Fig. 3.

one subject to the other, making the overall pattern of the ACF significantly different and hence could be used in gait recognition.

C. The Level Crossing Rate

Another manner of quantifying periodic signals is using the level crossing rate (LCR), which is the measure of how often a signal crosses a certain threshold going in a positive direction [20]. LCR represent signals in such a way that the primary focus is on power levels and frequency of crossing them. It clearly shows the signal range, and emphasizes the location of the high-frequency component of the signal. Fig. 6 shows the LCR representation of the signals shown in Fig. 3. As expected the LCR of the 3 subjects are different due to the difference in the subjects' gait, and the size of there bodies. The LCR show clearly the minimum and the maximum power level received by each subject. LCR could be too simple as a differentiating factor on its own, however, it could have good contribution as an additional feature.

III. Classification Learners

Four different classification learners were considered for distinguishing from the walking pattern of one person to the other based on extracted radio features discussed in Section II. The radio features are presented by a vector with a length L, taken from a period of 3 seconds. The vector length L, varies with the feature in hand where for time series $L = 600$, for ACF $L = 300$, and for LCR $L = 60$. All the classification learners are implemented in MATLAB environment with a brief introduction of each following in this section.

A. Decision Trees

Decision tree learners comprise a series of logical decisions taken at decision nodes, in which each possible decision's choice results in a tree branch. The tree is terminated by the leaf nodes that denote the result of following a combination of decisions. Data that is to be classified begin at the root node, where it is passed through the various decisions in the tree according to the values of its features, until it reaches a leaf node, which assigns it a predicted class [21]. To identify which feature to split upon at the decision nodes, Gini's diversity index was used as a split criterion. For a data set S, Gini index G is defined as follows [22]:

$$G(S) = 1 - \sum_{i=0}^{C-1} \left(\frac{s_i}{S}\right)^2 \tag{3}$$

where C is the number of predefined classes, and s_i is the number of samples belonging to class c_i. The quality of a split on a feature into h subsets S_j is then computed as the weighted sum of the Gini indices of the resulting subsets:

$$G_{split} = \sum_{j=0}^{h-1} \frac{n_j}{n} G(S_j) \tag{4}$$

where n_j is the number of samples in subset S_j after splitting, and n is the total number of samples in the given decision node. Thus, G_{split} is calculated for all possible features, and the feature with minimum value is selected as a split point. To limit the growth of the tree, so that the model does not get over-fitted to the training data, the maximum number of splits was set to 100. Detailed description of the decision tree classification learner is found in [21], [22].

B. Support Vector Machine

Support vector machine (SVM) is a type of machine learning algorithm in which the classification of the outputs depend on explicit generalization, obtained from analyses of the training data. In this algorithm, the training data items are put in a P-dimensional space, and classification is performed by finding the hyper-planes that differentiate the required number of classes very well. The obtained hyper-planes are then used in the classification of test data. The hyper-planes are obtained by maximizing functional margin which is the distances between the nearest data point and the hyper-plane. This can be achieved by [23]:

$$\min_{u,b} H(u) = \frac{||u||^2}{2} \text{ subject to } c_l(u^T p_l + b) \geq 1 \quad \text{for } l = 1, ..., P \tag{5}$$

where p_l is the training example, c_l represents the labels of the training examples, P is the total number of features to be compared, u is the weight vector and b is the bias of the optimal hyper-plane. The SVM can be extended to non-linear classification by the usage of kernel method to map the inputs into high-dimensional feature space. In this work, a quadratic kernel function was used in the application of SVM. See [23] for more details on the SVM classification learner.

C. K-Nearest Neighbors Classifier

k-nearest Neighbors (k-NN) algorithm is a type of machine learning algorithm in which the classification of the output does not depend on explicit generalization, but instead compares new problem instances with instances seen in training. More specifically, it compares the new problem with k nearest neighbors, and assign it to the class most common among them [24]. It is among the simplest of all machine learning algorithms especially in its simplest form where $k = 1$. The nearest neighbors are identified by calculating the Euclidean distance d between a training data p_l and the test data q_l as

$$d = \sqrt{\sum_{l=1}^{l=P} (p_l - q_l)^2} \tag{6}$$

Since (6) is dependent on how features are measured, the features values were re-scaled so that each one contributes relatively equally to the distance formula [25]. The algorithm was implemented with $k = 10$, in which weight v were assigned to the contributions of the neighbors using,

$$v = \frac{1}{d^2} \tag{7}$$

so that the nearer neighbors contribute more to the decision. A detailed description of the k-NN classification learner is found in [24], [25].

D. Artificial Neural Network

An Artificial Neural Network (ANN) models the relationship between a set of input data and the output class by the use of network of nodes known as artificial neurons to solve learning problems. Each node takes M inputs of r_m, weight them with w_m according to their importance, and then the summation is passed on according to an activation function $f(g)$. Mathematically the processes can be represented by the formula [21]:

$$y(x) = f\left(\sum_{m=1}^{M} w_m r_m\right) \tag{8}$$

with a sigmoid activation function defines as:

$$f(g) = \frac{1}{1 + e^{-g}} \tag{9}$$

The nodes were grouped into 2 layers, hidden layer, and output layer. The hidden layer processes the input data prior to reaching the output layer which does further processing and generates a final prediction. The number of nodes in the output layer is predetermined by the number of classes in the outcome, however, in the hidden layer, there is no reliable rule to determine the number of nodes needed. In this work, 25 nodes were used in the hidden layer as the addition of more nodes in this layer did not give significant improvement in performance. The weights w_m were adjusted in the training process using scaled conjugate gradient back-propagation algorithm. In this algorithm, the gradient of activation function is used to determine which weight should be adjusted in order to reduce the error between the actual and predicted class. See [21], [25] for more details on the ANN classification learner.

Fig. 7. Wearable radio transceiver. The device is approximately 50 mm x 20 mm x 20 mm.

TABLE I. VOLUNTEERS DETAILS

#	Gender	Age	Height (cm)	Weight (kg)
01	Female	35	168	63
02	Female	23	174	69
03	Female	25	159	53
04	Female	29	171	66
05	Female	24	167	61
06	Male	29	180	83
07	Male	35	185	75
08	Male	25	178	67
09	Male	23	173	80
10	Male	27	168	65
11	Male	28	183	105
12	Male	26	165	66
13	Male	30	160	53
14	Male	21	175	80
15	Male	30	181	75
16	Male	26	175	83
17	Male	26	167	79
18	Male	49	178	75
19	Male	40	170	78
20	Female	60	170	75

IV. EXPERIMENTAL DATA AND ANALYSIS

A. Measurement Data

The experiments conducted in this study are preliminary towards the validation of the proposed method. The dataset used to evaluate the RSSI-based gait recognition consist of 20 healthy subjects (14 males and 6 females), with different age, height, and weight detailed in Table I. During the data collection phase, 3 transceivers were attached on the participants, a transmitter on the right side of the waist representing devices such as smartphones, and a receiver on the wrist of the right and left arms representing devices such as smartwatches. The transceivers were attached in such a way that the antennas were vertically polarized. The participants were asked to walk at their normal speed in both outdoor and indoor environments in order to capture the influence of different environment. The outdoor environment was a parking lot with an asphalt surface, while the indoor environment was a cafeteria with a tiled surface. Each participant walked for approximately 4 minutes outdoors followed by 4 minutes indoors to include natural gait changes over time and environments. The experiments were limited to single trial per subject, with no donning/doffing of the transceivers. The transceivers (see Fig. 7) were made

using programmable radio CC2500 from Texas Instruments [26]. The transmitter was set to transmit a packet every 5 ms with constant transmission power of 1 dBm at the 2.425 GHz carrier frequency. The receiver was used to store the packet number together with RSSI on its MicroSD memory card. The data were later exported from the memory card to a computer running MATLAB software for analysis.

In MATLAB, the collected data was split into segments of 3 seconds giving us a total of 150 segments from each subject. In each segment, 3 radio channel features (time series, ACF, and LCR) discussed in Section II were extracted. The radio features were later used with classification learners discussed in Section III for testing the performance of the RSSI-based gait authentication system. For the case of time series, the signal was shifted on time axis so that all the segments have their peaks at $t = 0$ as in Fig 3. Whenever ACF was used as a radio feature, an additional process of eliminating segments with periodicity noise was used. The process was set to eliminated any segment in which its ACF does not have a peak greater than 0.3 at $\tau = 1$ period.

B. Performance Metric Index

A reliable gait authentication algorithm has to make a decision whether the gait measured is of the genuine user or an imposter. The following 3 success criteria could be used to measure its performance [9].

- **True positive rate (TPR)**: Also know as sensitivity, is the probability that the authentication system correctly accepts the access request from the genuine users. If TP and FN represents the number of times the genuine user's access request is accepted and rejected respectively, then TPR can be calculated as follows

$$\text{TPR} = \frac{\text{TP}}{\text{TP} + \text{FN}} \times 100 \tag{10}$$

- **True negative rate (TNR)**: Also known as specificity, is the probability that the authentication system correctly rejects the access request from an imposter. If TN and FP represents the number of times an imposter's access request is rejected and accepted respectively, then TNR can be calculated as follows

$$\text{TNR} = \frac{\text{TN}}{\text{TN} + \text{FP}} \times 100 \tag{11}$$

- **Recognition accuracy**: It represents the percentage of correct classifications which is simply the number of true classifications (acceptance from genuine users and rejection from imposter) over the total number of tests. It can be calculated as follows

$$\text{Accuracy} = \frac{\text{TP} + \text{TN}}{\text{TP} + \text{FN} + \text{TN} + \text{FP}} \times 100 \tag{12}$$

In general, the system should minimize the FPs and FNs, however, greater emphasis could be set on minimizing FPs so that the imposter's access request is rejected all the times.

TABLE II. PERFORMANCE RESULTS USING DATA FROM ONE RADIO CHANNEL: RIGHT WRIST TO WAIST

Radio feature	Performance metric	Decision tree	Quadratic SVM	Weighted k-NN	ANN
TS	TPR	67%	86%	83%	68%
	TNR	67%	88%	85%	71%
	Accuracy	70%	88%	85%	74%
ACF	TPR	63%	81%	72%	85%
	TNR	64%	84%	77%	86%
	Accuracy	66%	83%	75%	86%
LCR	TPR	57%	70%	64%	73%
	TNR	56%	72%	67%	74%
	Accuracy	61%	74%	67%	76%
TS+ACF	TPR	77%	92%	87%	90%
	TNR	76%	93%	89%	91%
	Accuracy	78%	93%	89%	91%
TS+LCR	TPR	71%	89%	86%	85%
	TNR	71%	89%	88%	85%
	Accuracy	73%	89%	88%	87%
ACF+LCR	TPR	72%	88%	81%	93%
	TNR	72%	90%	85%	94%
	Accuracy	73%	90%	84%	94%
TS+ACF+LCR	TPR	76%	92%	89%	94%
	TNR	76%	93%	91%	95%
	Accuracy	78%	93%	91%	95%

C. Results and Discussions

The objective of the analysis is to investigate which radio channel feature and which classification leaner are suitable for RSSI-based gait authentication system. For each radio channel feature obtained from the channel between the right wrist and the waist, the performance of each classification learner in terms of TPR, TNR, and accuracy is evaluated independently, and in combination with each other. The same analysis were repeated when additional radio features were extracted from the channel between the left wrist and the waist, and used together with those from the channel between the right wrist and the waist. From our experimental data, 150 of 3-second segments were extracted from each user, giving us a total of 2550 segments for testing. To protect the algorithm against over-fitting, a 10 folds cross-validation method was employed. In this method, the data set is partitioned into 10 fold, in which 9 are used for training and 1 is used for validation purposes. The training and testing process is repeated 10 times so that each of the 10 partition is used exactly once as the testing data. The results are then averaged over the 10 validations to yield the average performance.

Table II and Fig. 8 show the performance of the different classifiers using time series (TS), ACF, LCR, and different combination of those features, obtained from radio channel between the right wrist and the waist. For all the radio features, the worst performance is shown by decision tree algorithm, with maximum accuracy of 78% obtained when all the radio features are used together. When only a single radio feature is used, LCR has shown to give the worst results, and TS the best results for all classification learners except ANN, in which TS gave the worst results and ACF gave the best results. When the radio features are used in pairs, ACF+LCR pair gives the best results when ANN is used, while TS+ACF pair gives the best results for the remaining classification learners. The combination of all 3 features archives an accuracy of 95% using ANN as the classification learner. It is also interesting

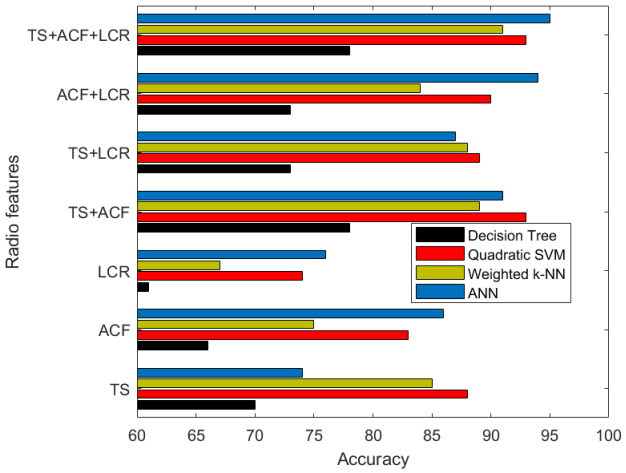

Fig. 8. Performance results using data from one radio channel: Right wrist to waist.

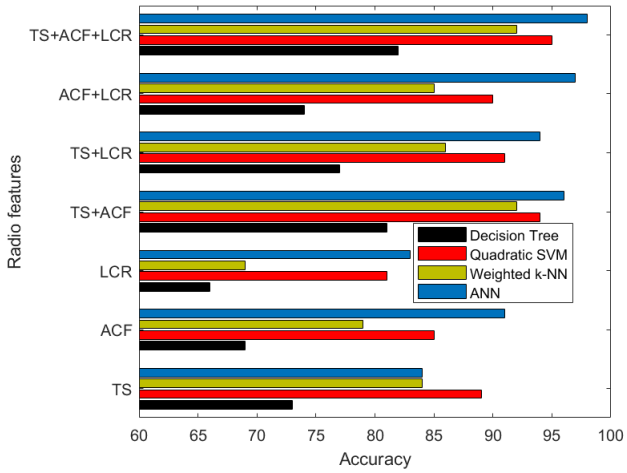

Fig. 9. Performance results using data from two radio channels: Right wrist to waist, and left wrist to waist.

TABLE III. PERFORMANCE RESULTS USING DATA FROM TWO RADIO CHANNELS: RIGHT WRIST TO WAIST, AND LEFT WRIST TO WAIST

Radio feature	Performance metric	Decision tree	Quadratic SVM	Weighted k-NN	ANN
TS	TPR	69%	88%	81%	81%
	TNR	69%	89%	83%	83%
	Accuracy	73%	89%	84%	84%
ACF	TPR	66%	82%	75%	90%
	TNR	66%	85%	82%	91%
	Accuracy	69%	85%	79%	91%
LCR	TPR	62%	78%	64%	81%
	TNR	63%	81%	69%	81%
	Accuracy	66%	81%	69%	83%
TS+ACF	TPR	78%	93%	90%	95%
	TNR	78%	94%	92%	96%
	Accuracy	81%	94%	92%	96%
TS+LCR	TPR	75%	89%	84%	93%
	TNR	75%	90%	87%	93%
	Accuracy	77%	91%	86%	94%
ACF+LCR	TPR	72%	88%	83%	96%
	TNR	72%	90%	86%	96%
	Accuracy	74%	90%	85%	97%
TS+ACF+LCR	TPR	79%	94%	90%	98%
	TNR	79%	94%	92%	98%
	Accuracy	82%	95%	92%	98%

to notice that, moving from the use of a single radio feature (TS with SVM as classification learner) to radio features in pair (ACF+LCR pair with ANN as a classification learner) improves accuracy by 6%, while from the pair to the combination of all 3 radio features (TS+ACF+LCR with ANN as the classification learner) the improvement is only 1%.

When additional radio features are extracted from the channel between the left wrist and the waist, and are used together with those from the channel between the right wrist and the waist, we notice improvement in all performance metric (see Table III and Fig. 9), with the most improvement in accuracy of 7% achieved when LCR is used as a single radio feature, and the least of 1% achieved when TS is used as a single radio feature. We also notice a similar trend in which moving from the use of a single radio feature (ACF with ANN as classification learner) to a pair of features (ACF+LCR pair with ANN as classification learner) accuracy improves by 6%, while from the pair to the combination of all 3 radio features (TS+ACF+LCR with ANN as classification learner) only 1% of improvement is achieved. Here the accuracy reaches 98%.

Based on the above results, the use of ACF+LCR pair, extracted from a single radio channel, with ANN as the classification learner is suggested for practical implementations. This is due to the level of accuracy achieved (94%), despite the number of predictors being 67% less than those used to achieve the best performance. Its confusion matrix is shown in Fig. 10 with positive predictive values in green, and the false discovery rates highlighted in red.

V. CONCLUSION

In this study, an RSSI-based gait authentication algorithm was proposed. The system is applicable when unobtrusive, natural method of authentication, with low hardware cost and power demands is needed. The system was based on extracting features from the radio channels between the wrists and the waist, through RSSI present in all wireless devices. The features extracted were time series, ACF, and LCR from 20 subjects walking in outdoor and indoor environment. Four different classification learners namely decision tree, SVM, k-NN, and ANN were used for testing of the algorithm.

The overall best performance was achieved using all the radio features together (TS+ACF+LCR), extracted from 2 radio channels, right wrist to waist, and left wrist to waist, and using ANN as the classification learner. All the performance metric namely TPR, TNR, and accuracy were above 97%, see Table III. In a more practical approach, where the radio features were extracted from just 1 radio channel (right wrist to waist), the best performance achieved was above 95% for all performance metric, while using all the radio features, with ANN as the classification learner. This suggests that RSSI-based authentication system could be based on just 2 devices, (for example a smartwatch and a smartphone) especially when

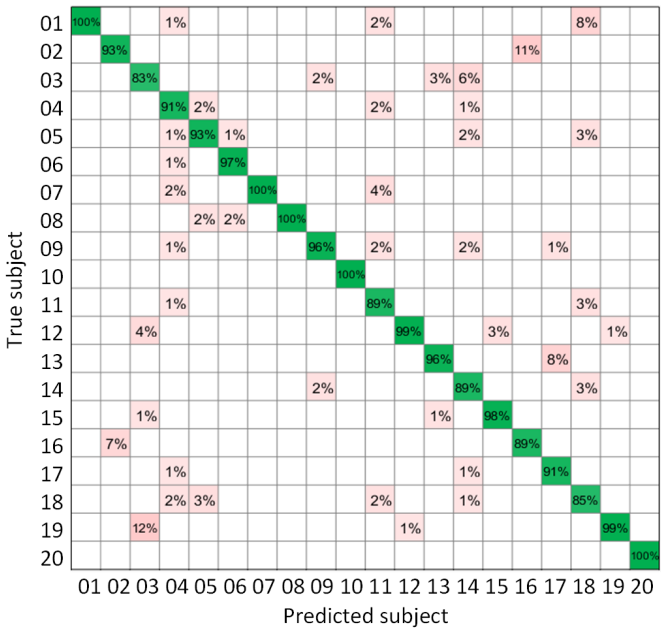

Fig. 10. Confusion matrix showing positive predictive values in green, and false discovery rates in red. The radio features used were ACF+LCR with ANN as the classification learner.

the system is used as a complementary to other security features.

In general the RSSI-based authentication method, using a pair of ACF+LCR extracted from a single radio channel, with ANN as the classification learner, achieved a good level of accuracy (94%), with comparatively small number of predictors (67% less than the best performer), and hence has a good potential for practical implementation.

REFERENCES

[1] R. Cavallari, F. Martelli, R. Rosini, C. Buratti, and R. Verdone, "A survey on wireless body area networks: Technologies and design challenges," *IEEE Communications Surveys & Tutorials*, vol. 16, no. 3, pp. 1635–1657, 2014.

[2] N. Zhao, A. Ren, M. U. Rehman, Z. Zhang, X. Yang, and F. Hu, "Biometric behavior authentication exploiting propagation characteristics of wireless channel," *IEEE Access*, vol. 4, pp. 4789–4796, 2016.

[3] J. Andreu-Perez, D. R. Leff, H. M. Ip, and G.-Z. Yang, "From wearable sensors to smart implants—toward pervasive and personalized healthcare," *IEEE Transactions on Biomedical Engineering*, vol. 62, no. 12, pp. 2750–2762, 2015.

[4] Y. Zhang, G. Pan, K. Jia, M. Lu, Y. Wang, and Z. Wu, "Accelerometer-based gait recognition by sparse representation of signature points with clusters," *IEEE Transactions on Cybernetics*, vol. 45, no. 9, pp. 1864–1875, 2015.

[5] R. Ferrero, F. Gandino, B. Montrucchio, M. Rebaudengo, A. Velasco, and I. Benkhelifa, "On gait recognition with smartphone accelerometer," in *Proceeding of 4th Mediterranean Conference on Embedded Computing (MECO)*, 2015, pp. 368–373.

[6] J.-H. Wang, J.-J. Ding, Y. Chen, and H.-H. Chen, "Real time accelerometer-based gait recognition using adaptive windowed wavelet transforms," in *Proceeding of IEEE Asia Pacific Conference on Circuits and Systems (APCCAS)*, 2012, pp. 591–594.

[7] C. Nickel and C. Busch, "Does a cycle-based segmentation improve accelerometer-based biometric gait recognition?" in *Proceedings of 11th International Conference on Information Science, Signal Processing and their Applications (ISSPA)*, 2012, pp. 746–751.

[8] M. Muaaz and C. Nickel, "Influence of different walking speeds and surfaces on accelerometer-based biometric gait recognition," in *Proceedings of 35th International Conference on Telecommunications and Signal Processing (TSP)*, 2012, pp. 508–512.

[9] W. Xu, G. Lan, Q. Lin, S. Khalifa, N. Bergmann, M. Hassan, and W. Hu, "KEH-gait: Towards a mobile healthcare user authentication system by kinetic energy harvesting," in *Proceedings of NDSS*, 2017.

[10] Z. Nie, Y. Liu, C. Duan, Z. Ruan, J. Li, and L. Wang, "Wearable biometric authentication based on human body communication," in *Proceedings of IEEE 12th International Conference on Wearable and Implantable Body Sensor Networks (BSN)*, 2015, pp. 1–5.

[11] Y. Li and T. Zhu, "Using Wi-Fi signals to characterize human gait for identification and activity monitoring," in *Proceedings of IEEE First International Conference on Connected Health: Applications, Systems and Engineering Technologies (CHASE)*, 2016, pp. 238–247.

[12] Q. Xu, Y. Chen, B. Wang, and K. R. Liu, "Radio biometrics: Human recognition through a wall," *IEEE Transactions on Information Forensics and Security*, vol. 12, no. 5, pp. 1141–1155, 2017.

[13] C. Shi, J. Liu, H. Liu, and Y. Chen, "Smart user authentication through actuation of daily activities leveraging WiFi-enabled IoT," in *Proceedings of the 18th ACM International Symposium on Mobile Ad Hoc Networking and Computing*, 2017, p. 5.

[14] S. Ullah, H. Higgins, B. Braem, B. Latre, C. Blondia, I. Moerman, S. Saleem, Z. Rahman, and K. S. Kwak, "A comprehensive survey of wireless body area networks," *Journal of medical systems*, vol. 36, no. 3, pp. 1065–1094, 2012.

[15] S. A. Salehi, M. Razzaque, I. Tomeo-Reyes, and N. Hussain, "IEEE 802.15.6 standard in wireless body area networks from a healthcare point of view," in *Proceedings of 22nd Asia-Pacific Conference on Communications (APCC)*, 2016, pp. 523–528.

[16] F. Büsching, U. Kulau, M. Gietzelt, and L. Wolf, "Comparison and validation of capacitive accelerometers for health care applications," *Computer Methods and Programs in Biomedicine*, vol. 106, no. 2, pp. 79–88, 2012.

[17] B. Priyantha, D. Lymberopoulos, and J. Liu, "Littlerock: Enabling energy-efficient continuous sensing on mobile phones," *IEEE Pervasive Computing*, vol. 10, no. 2, pp. 12–15, 2011.

[18] S. Van Roy, F. Quitin, L. Liu, C. Oestges, F. Horlin, J.-M. Dricot, and P. De Doncker, "Dynamic channel modeling for multi-sensor body area networks," *IEEE Transactions on Antennas and Propagation*, vol. 61, no. 4, pp. 2200–2208, 2013.

[19] L. Hanlen, V. Chaganti, B. Gilbert, D. Rodda, T. Lamahewa, and D. Smith, "Open-source testbed for body area networks: 200 sample/sec, 12 hrs continuous measurement," in *Proceedings of IEEE 21st International Symposium on Personal, Indoor and Mobile Radio Communications Workshops (PIMRC Workshops)*, 2010, pp. 66–71.

[20] T. S. Rappaport *et al.*, *Wireless Communications: Principles and Practice*. prentice hall PTR New Jersey, 1996, vol. 2.

[21] B. Lantz, *Machine Learning with R*. Packt Publishing Ltd, 2015.

[22] M. Kantardzic, *Data Mining: Concepts, Models, Methods, and Algorithms*. John Wiley & Sons, 2011.

[23] N. Cristianini and J. Shawe-Taylor, *An Introduction to Support Vector Machines and Other Kernel-Based Learning Methods*. Cambridge university press, 2000.

[24] N. S. Altman, "An introduction to kernel and nearest-neighbor nonparametric regression," *The American Statistician*, vol. 46, no. 3, pp. 175–185, 1992.

[25] M. N. Murty and V. S. Devi, *Pattern Recognition: An Algorithmic Approach*. Springer Science & Business Media, 2011.

[26] T. Instruments, "CC2500 low-cost low-power 2.4 GHz RF transceiver," *Data Sheet*, 2011.